



Comparison of boron removal by ion-exchange resin in column and hybrid membrane process

Assma Alharati, Yousef Swesi, Koffi Fiatty, Catherine Charcosset*

Univ Lyon, Université Claude Bernard Lyon 1, CNRS, LAGEP UMR 5007, 43 boulevard du 11 novembre 1918, F-69100, Villeurbanne, France, Tel. +33 4 72 43 18 34; emails: catherine.charcosset@univ-lyon1.fr (C. Charcosset), assma-ahmed.al-harati@etu.univ-lyon1.fr (A. Alharati), swy@lgpc.cpe.fr (Y. Swesi), koffi.fiatty@univ-lyon1.fr (K. Fiatty)

Received 1 March 2018; Accepted 9 July 2018

ABSTRACT

Ion exchange is a major technique for boron removal from seawater using specific ion-exchange resins. The aim of this study was to compare two techniques using ion-exchange resins (column and hybrid ion-exchange microfiltration) for boron removal. For that, model boron solutions were used and ion-exchange resin with different size (unsieved, sieved at 500 and 600 μm , ground and sieved at 40 and 60 μm) for three commercial resins (Amberlite IRA743, Diaion CBR05, Purolite S108) in batch, column, and in an hybrid ion-exchange/microfiltration system. In batch, an important increase in kinetics was observed for smaller resins (40–60 μm and <500 μm). In column, delayed and sharper breakthrough curves were observed for resins with size <500 μm . With the hybrid system, the breakthrough curve observed at optimal conditions and the 40–60 μm Amberlite IRA743 resin was similar to the one obtained in a column with the <500 μm resin; however, the flow rate with the hybrid system was 20 times higher. Overall, the resin size had a major effect on the ion-exchange resin efficacy for boron removal, and the ion-exchange resin/microfiltration process that uses resins with much smaller size is promising.

Keywords: Boron removal; Ion-exchange resin; Column; Breakthrough curve; Hybrid membrane process

1. Introduction

Desalination is implemented worldwide to respond to the increasing need of freshwater for both human consumption and culture irrigation. Reverse osmosis using appropriate membranes with very small pore size is a major technique for desalination. Despite its success, it suffers from some drawbacks, one of them being the high boron concentration in the water obtained. Indeed, boron is vital for the growth of plants at small concentration, but has negative effects at higher concentration. In general, boron concentration in irrigation water should not exceed 0.3–4 mg/L depending on the plant and soil characteristics [1]. For humans, high boron concentration leads to negative effects such as malfunctioning of the cardiovascular, alimentary, reproduction, and nervous system

[1,2]. Although the World Health Organization has increased the recommended maximum concentration (from 0.3 to 0.5 and 2.4 mg/L in 2011 [3]), high boron concentration remains a problem, and additional processes have to be added to reverse osmosis plants. Several techniques are available for boron removal such as ion exchange, reverse osmosis, chemical precipitation, adsorption, and electrocoagulation [1,2,4], the most popular technique uses ion-exchange resins specifically designed for boron removal. These commercial resins (e.g., Amberlite IRA743, Purolite S108, and Diaion CR05) have a macroporous polystyrene matrix on which *N*-methyl-*D*-glucamine functional groups are attached. Boron is then retained according to the following reaction scheme: borate ion is complexed by two sorbitol groups, and a proton is retained by a tertiary amine site that behaves as a weakly basic anion exchanger [5].

* Corresponding author.

Boron removal by ion-exchange resin in batch system was investigated by several authors to evaluate the effect of several parameters (e.g., resin dosage, contact time, boron concentration, solution pH/temperature, and side ions) on sorption kinetics and isotherms [5–9]. The kinetics of boron binding onto ion-exchange resins was described by models, for example, the pseudo-first and pseudo-second-order models [8]. Besides, ion-exchange resins in columns were tested to investigate the effect of several parameters (bed volume [BV] of resin, flow rate, boron concentration, etc.) on breakthrough curves [6,10–12]. A comparative study of commercial resins was carried out in a pilot plant [13]. Models were also proposed to represent the experimental breakthrough curves such as Thomas and Yoon-Nelson models [8]. In order to demonstrate the reusability of the ion-exchange resin, sorption–elution–washing–regeneration–washing cycles were repeated several times [14]. Boron removal in batch or in column was applied to the treatment of synthetic waters, geothermal water [12], permeate obtained from seawater reverse osmosis [6,11] and wastewater [10,15].

Ion-exchange resins were also used in a hybrid process in which a reactor is associated to a microfiltration (MF) membrane (submerged or not) [16–18]. In most configurations, boron solution and fresh resin are continuously added to the reactor, while saturated resins are removed at the same flow rate by MF [18,19]. The technique can also be performed without continuous addition of resin [20,21]. Ion-exchange resin with small size is used to increase the kinetics of sorption, consequently boron is retained before passing in the permeate. The major advantages of the technique are that the kinetics and process efficiency are increased. Several parameters were tested (e.g., boron concentration, flow rate, membrane type, etc.), and the process was investigated for boron removal from model boron solution [17,20,21], seawater [17], and geothermal water [18,19].

The use of resin of small size is therefore essential for the hybrid ion-exchange/MF technique. In batch, the effect of resin size on boron removal is also crucial. Indeed, Kabay et al. [6] compared the adsorption isotherm and kinetics of ground and original resins Diaion CRB02 and Dowex XUS 43594.00. The size of the ground resin was in the range of 45–75 μm and the unground resin between 355 and 500 μm . The kinetics of the ground resin was found much faster than the unground one, this result being explained by the increase in surface area. Moreover, Darwish et al. [9] studied the effect of resin size in batch. Boron removal from water with fractions of Amberlite IRA743 resin of different particle sizes of 1–45, 150–180, and 500–700 μm was studied. The values of boron removal from water after 2 h in batch reached 75.4%, 48.2%, and 15.0% for the resin fractions with particle sizes of 1–45, 150–180, and 500–700 μm , respectively. Although such a crucial effect has been observed in batch, the effect of resin size is much less investigated in a column or in the hybrid process.

In this study, we compared boron removal by ion-exchange resin for several configurations: batch, column, and hybrid ion-exchange/MF. To obtain resins of different size, the original resins were sieved, while to obtain resins with smaller size (40–60 μm), the resins were ground before sieving. The smallest resins (40–60 μm) were not used in the column due to the high pressure generated, but in the hybrid process where the transmembrane pressure driving

the process is much lower. The two processes were then compared by measuring the boron concentration vs. BV divided by the amount or volume of resin used. The hybrid process was conducted without resin addition as usually performed, which may present several advantages such as easier maintenance and better use of the resin capacity. In addition, the hybrid ion-exchange/MF process was compared with a column, bringing new insights in the understanding of these techniques of boron removal.

2. Materials and methods

2.1. Chemicals

Three commercial ion-exchange resins were tested: Amberlite IRA743 (Sigma-Aldrich, France), Purolite S108 (Purolite, France), and Diaion CRB05 (Resindion, Italy). These resins are specifically used for boron removal and have similar characteristics. In particular, they are all made from crosslinked macroporous polystyrene, with the active group *N*-methyl-*D*-glucamine.

Boric acid (99.97%) was supplied by Sigma-Aldrich (France). Boric acid solutions were prepared by dissolving 0.751 g of boric acid in 1 L of demineralized water, the concentration of this solution being 100 mg/L. Solutions at 5 mg/L were obtained from this stock solution.

For the regeneration of the membrane, hydrochloride acid (HCl 37%) and sodium hydroxide (NaOH \geq 98%) were supplied by Sigma-Aldrich (France). For the analysis of boron concentration, azomethine-H and other reactants were supplied by Sigma-Aldrich (France).

2.2. Preparation and characterization of ion-exchange resins

Ion-exchange resins were tested in a column and in the hybrid ion-exchange/MF process. In the column, the resins used were obtained by sieving on a vibratory sieve shaker (AS200, Retsch, France) with sieves of 500 and 600 μm . In the hybrid process, smaller Amberlite IRA743 resins were used. They were obtained by grounding the initial resin using a planetary ball mill (PM 100, Retsch, France), followed by sieving on 40 and 60 μm sieves.

The resin size distributions were obtained using a Mastersizer 3000 (Malvern, France). The Mastersizer instrument measures the intensity of scattered light as a laser beam passes through a sample of dispersed particles. The Brunauer-Emmett-Teller (BET) theory surface areas of the resins were determined with a surface area analyzer TriStar 3000 (Micromeritics, France).

2.3. Batch experiments

Kinetic experiments were performed in batch during 24 h. For that, 1 g of resin was added to 500 mL of boron solution at 5 mg/L in a 1,000 mL beaker. The resin dosage was then 2 g/L. The suspension was stirred continuously using a mechanic stirrer (RW 20, IKA-Werke, France) at 200 rpm. The pH of the suspension was adjusted to 8.2, to be close to the pH of seawater pH, by adding droplets of NaOH (1 M). The pH was measured with a SevenMulti pH meter (Mettler Toledo, France). The temperature was maintained at 25°C using a thermostated bath. At regular time intervals, 1 mL

of samples were taken out from the suspension and filtered with 0.45 μm pore size cellulose acetate Millex filters (Merk, France). Boron concentrations in the filtrate samples were then obtained using the azomethine-H method [22]: after adding appropriate reactants, the adsorbance was measured at 420 nm with a visible–UV spectrophotometer Cary 50 Probe (Agilent Technologies, France).

2.4. Column experiments

The experimental setup used for the column experiments is shown in Fig. 1. A low-pressure chromatography setup Äktaprime Plus chromatography system (GE Healthcare Life Sciences, France) was used with a fraction collector. Before loading the boron solution, 2 g of resin was packed in a glass column (internal diameter 1 cm, height 9 cm) and washed with deionized water. BVs of resins are indicated in Table 1. For all experiments, the flow rate was set to 2 mL/min. From the outlet of the column, each successive fractions of effluent were collected using the fraction collector. Breakthrough curves were obtained by analysis of each fraction using the azomethine-H method. A pressure transducer at the column inlet gave the inlet pressure.

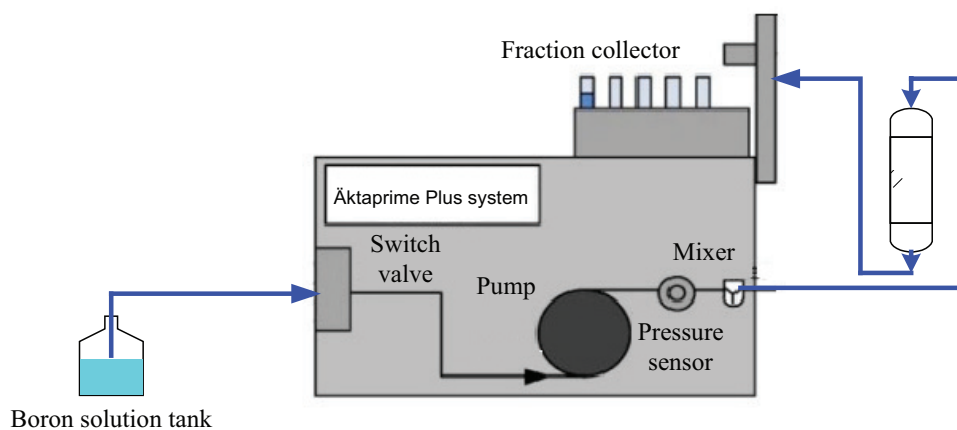


Fig. 1. Experimental setup for the column experiments.

Table 1
Characteristics of the various resins (original, sieved, ground, and sieved)

Resins	d_{10} (μm)	d_{50} (μm)	d_{90} (μm)	Span (-)	Specific area (m^2/g)	V (mL) for 2 g
Amberlite IRA743 original	451	565	720	0.476	24.3	3.8
Amberlite IRA743 <500 μm	386	456	541	0.338	23.9	5
Amberlite IRA743 500–600 μm	480	553	638	0.285	23.9	3.5
Amberlite IRA743 >600 μm	557	668	805	0.371	21.8	3.3
Amberlite IRA743 40–60 μm	30.7	44.6	64.2	0.750	26.6	4.6
Purolite S108 original	430	528	645	0.407	^a	4.3
Purolite S108 <500 μm	406	469	543	0.291	^a	4.6
Purolite S108 >500 μm	489	576	673	0.320	^a	3.6
Diaion CRB05 original	335	624	919	0.685	23.2	3.3
Diaion CRB05 <500 μm	347	427	527	0.422	21.2	3.2
Diaion CRB05 500–600 μm	477	562	656	0.319	20.2	3.4
Diaion CRB05 >600 μm	595	727	904	0.426	19.7	3.1

^a Unreliable data were obtained for the specific area of the Purolite S108 resins.

2.5. Sorption/MF setup

For the sorption/MF experiments, the experimental setup included a Micro Kerasep® membrane device (Novasep, France) as shown in Fig. 2. The boron solution was continuously added to a 3 L reactor using a Quattroflow 150S pump (Pall, France), while the resin suspension was recirculated in the MF loop using a Quattroflow 1000S pump (Pall, France). Two pressure gauges were placed at the inlet and outlet of the module, and a valve at the outlet for transmembrane pressure setting. A mechanic stirrer (RW 20, IKA-Werke, France) stirred the feed suspension of ion-exchange resin in the reactor at 200 rpm.

The Kerasep® ceramic membrane is tubular, with an outside diameter of 10 mm, an inner diameter of 6 mm, and a length of 40 cm; the active membrane area is, therefore, 0.0075 m^2 . The active layer is made of $\text{ZrO}_2\text{-TiO}_2$ deposited on a monolithic $\text{TiO}_2/\text{Al}_2\text{O}_3$ support. The membrane used had a 0.1 μm pore size.

2.6. Sorption/MF experiments

The sorption/MF experiments were conducted by delivering the boron solution in the reactor at the same flow rate

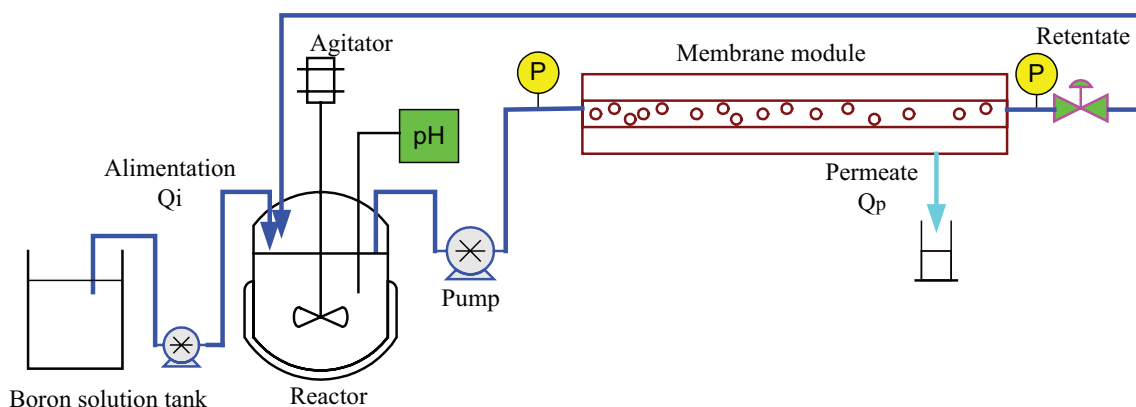


Fig. 2. Experimental setup of the ion-exchange/MF hybrid system; P , pressure gauge; Q_p , permeate flow rate; Q_i , inlet flow rate of the boron solution $Q_i = Q_p$.

as the permeate flow rate, to maintain a constant volume in the reactor. The process was operated in a closed-loop configuration, the suspension being continuously returned to the feed tank and the permeate being recovered. The feed flow rate was set to 5.45 L/min, corresponding to a mean tangential velocity of 3.2 m/s in the tubular membrane. The pH in the reactor was continuously measured using a SevenMulti pH meter (Mettler Toledo, France), and drops of NaOH 1 M were regularly added to maintain a pH value around 8.2. The temperature of the suspension in the reactor was set to 25°C. At regular time intervals, the permeate flow rate was measured. The permeate flux was obtained by dividing the flow rate by the membrane area. Permeate samples were collected at regular time intervals for analysis of boron concentration by the azomethine-H method [22].

After each experiment, the suspension of ion-exchange resin was removed by flushing the experimental setup with water in an open-loop configuration. The membrane and the experimental setup were then cleaned by flushing successively with acid (1.85% HCl), water, base (5% NaOH), and water in a closed-loop configuration and by removing the permeate. After each cleaning cycle, the membrane permeability was checked to be close to its initial value (more than 95%).

3. Results

3.1. Characterization of resins

The resins were fractionated into three fractions for the Amberlite IRA743 and Diaion CRB05 resins and two fractions for the Purolite S108 resin due to the sharper size distribution of this resin as detailed below. The resins were termed according to the sieve(s) used: with one sieve at 500 μm , the resins were termed <500 μm , with one sieve at 600 μm , the resins were named >600 μm , and for the resins obtained by using two sieves at 500 and 600 μm , the resins were termed 500–600 μm .

The size distribution of the three original resins is plotted in Fig. 3(a), and the size distributions of sieved and ground/sieved resins in Figs. 3(b)–(d), for the Amberlite IRA743, Diaion CRB05, and Purolite S108, respectively. Ground and sieved resins were only prepared with the Amberlite IRA 743 resins, for the two other resins, similar results were obtained (data not shown).

All resins were characterized for their size distribution, surface area, and BVs (Table 1). The particle size is given by d_{10} , d_{50} and d_{90} data, which represent, respectively, the cumulative volumetric fraction of particles at 10%, 50%, and 90%. The span value is obtained using Eq. (1) and is an indication of the particle size distribution [23]:

$$\text{span} = \frac{d_{90} - d_{10}}{d_{50}} \quad (1)$$

Low span values indicate a sharp distribution of particle size and higher span values correspond to a broader particle size distribution.

The three original resins showed higher span values than the sieved resins indicating larger size distributions. By comparing the original resins, the Diaion CRB05 had the highest span value (0.685) and the Amberlite IRA743 and Purolite S108 resins the lowest ones, respectively (0.476 and 0.407). This result is in agreement with the size distributions shown in Fig. 3(a). In particular, a small fraction with size around 200–300 μm was observed with the Diaion CRB05 resin but not for the two other resins. From Figs. 3(b) and (d), respectively, it appears clearly that the resins Amberlite IRA743 and Diaion CRB05 with 500–600 μm size gave a sharper size distribution, as they have been obtained by using two sieves. The sharper size distribution was obtained for the Purolite S108 resin (Fig. 3(c)). This explains why only two fractions were obtained by sieving (<500 and >500 μm). In addition, the ground and sieved Amberlite IRA743 resin (40–60 μm) had the highest span value (0.750). In this case, the d_{90} and d_{10} values were, respectively, equal to 64.2 and 30.7 μm , their difference being close to d_{50} (44.6 μm).

The BET surface areas of the Amberlite IRA743 and Diaion CRB05 resins are indicated in Table 1. For the Purolite S108 resin, unreliable data were obtained, which may be due to the presence of microporosities inside the resin. As expected, the surface area decreased with particle size. When comparing resins with the same size, the surface area was slightly lower for the Diaion CRB05 than the Amberlite IRA743 resin. Besides, the data obtained for the Amberlite IRA743 resin were in the range to those obtained by Darwish et al. [9,20] for different resin size (20–26 m^2/g).

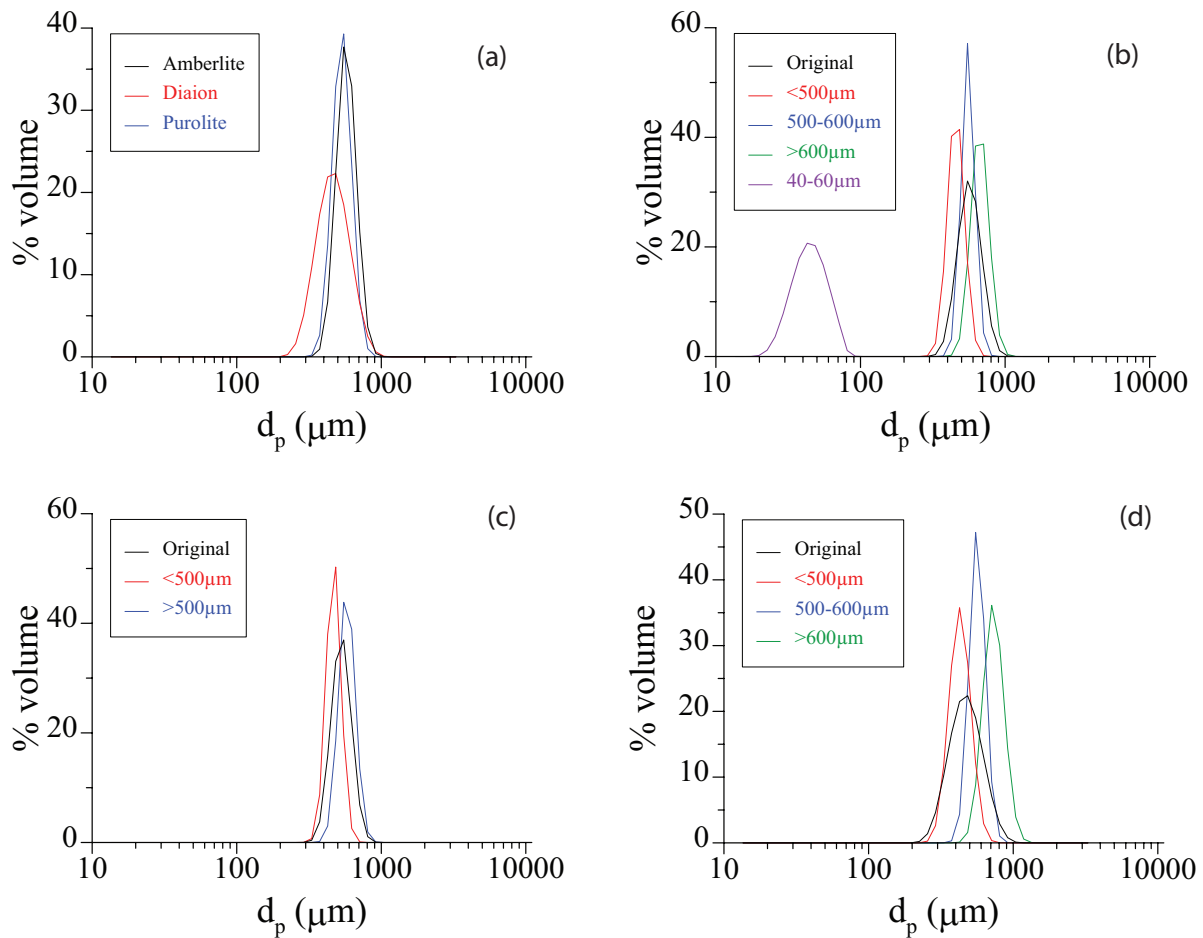


Fig. 3. Size distributions: (a) the three original resins; (b) Amberlite IRA743 resins with different size; (c) Purolite S108 resins with different size; and (d) Diaion CRB05 resins with different size.

The BVs of the various resins are also indicated in Table 1. The BVs were measured for 2 g of resin, which was the mass packed in the column. For the Amberlite IRA743 and Purolite S108 resins, the BVs decreased when increasing the resin size. For example, the BV of the Amberlite IRA743 resin was 5 mL and 3.3 mL for the <500 and >600 μm resin size, respectively. For the original resins, the BVs data were between the data of the smallest and largest resins. In addition, the ground and sieved Amberlite IRA743 resin had the highest BV (4.61 mL for 2 g of resin). However, a different behavior was observed for the Diaion CRB05 resin. Indeed, the BV of the resin with the smallest size of <500 μm (3.2 mL) was lower than the one of the 500–600 μm resin (3.4 mL), suggesting a different packing behavior than the Amberlite IRA743 and Purolite S108 resins. These different packing behaviors may be due, for example, to different surface properties.

3.2. Kinetics of boron sorption in batch

The ratio C/C_0 , C being the boron concentration in solution and C_0 the initial boron concentration, was measured vs. time. The kinetics of boron sorption for the three resins sieved at 500 μm (<500 μm resins) are shown in Fig. 4. Very little difference was observed between the three resins: boron removal was slightly faster for the Purolite S108 and Amberlite IRA743

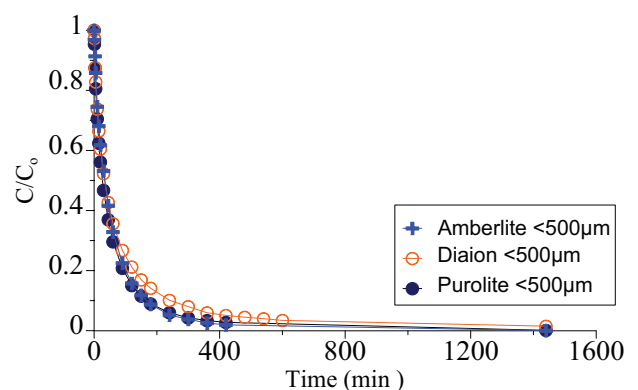


Fig. 4. Kinetics of three resins with particle size <500 μm .

resins than the Diaion CRB05 resin. For the Purolite S108 and Amberlite IRA743 resins, boron removal was complete after 24 h (0.005 mg/L), while a slightly higher amount of boron was still present in the solution with the Diaion CRB05 resin (0.11 mg/L). In the literature, similar kinetics was obtained for different commercial resins designed for boron removal. For example, Kabay et al. [6] reported very small differences between kinetics obtained with Dowex-XUS 43594.00 and Diaion CRB02 resins.

Boron concentration in solution against time was measured for the Amberlite IRA743 resins with four different sizes (Fig. 5). As shown, the kinetics was faster when decreasing the resin size. The much faster kinetics obtained with the smaller resin size is due to the higher surface area available (Table 1) and to the decrease of diffusion resistance in the smaller particles [6,9,11].

3.3. Influence of the size of the resin in a packed column

The boron fraction that passes through the resin column is equal to C/C_0 , C being the concentration in the effluent and C_0 being here the inlet concentration. The plot of C/C_0 vs. the number of BV (calculated as the volume of solution that passed through the column (mL solution)/mL resin) represents the breakthrough curve. The shape of the breakthrough curve is very important in determining the response of a column and in evaluating the efficiency of a sorbent [8]. The volume of water treated when boron begins to appear in the effluent is also an important parameter. Results obtained in the column experiments are summarized in Table 2. These data include the breakthrough volume (when the concentration 0.3 mg/L is reached at the column outlet) divided by the volume or mass of resin.

The breakthrough curves are plotted for the three ion-exchange resins Amberlite IRA743, Purolite S108 and

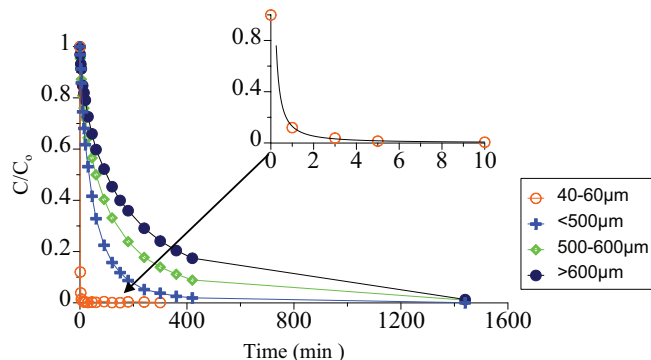


Fig. 5. Kinetics of the Amberlite IRA743 resins with different size.

Table 2
Results for boron removal with different resins packed in a column

Resins	Volume of resin for 2 g (mL)	Boron concentration at breakthrough (mg/L)	Volume treated at breakthrough/ volume resin BV	Time of treatment (min)	Volume treated at breakthrough (L)	Volume treated at breakthrough (L)/g resin
Amberlite IRA743 original	3.8	0.31	210	400	0.8	0.4
Amberlite IRA743 <500 µm	5	0.32	400	1,000	2	1
Amberlite IRA743 500–600 µm	3.5	0.24	200	350	0.7	0.35
Amberlite IRA743 >600 µm	3.3	0.35	150	250	0.5	0.25
Purolite S108 original	4.3	0.30	280	600	1.2	0.6
Purolite S108 <500 µm	4.6	0.30	370	850	1.7	0.85
Purolite S108 >500 µm	3.6	0.30	195	350	0.7	0.35
Diaion CRB05 original	3.3	0.30	315	600	1.2	0.6
Diaion CRB05 <500 µm	3.2	0.30	530	850	1.7	0.85
Diaion CRB05 500–600 µm	3.4	0.32	170	200	0.4	0.2
Diaion CRB05 >600 µm	3.1	0.25	60	100	0.2	0.1

Diaion CRB05, respectively, in Figs. 6–8. For the Amberlite IRA743 resin, three fractions were obtained by sieving: <500, 500–600, and >600 µm. Fig. 6 shows that the breakthrough curve of the original resin was identical to the one obtained with the resin of intermediate size (500–600 µm). For the <500 µm resin, breakthrough was delayed with a

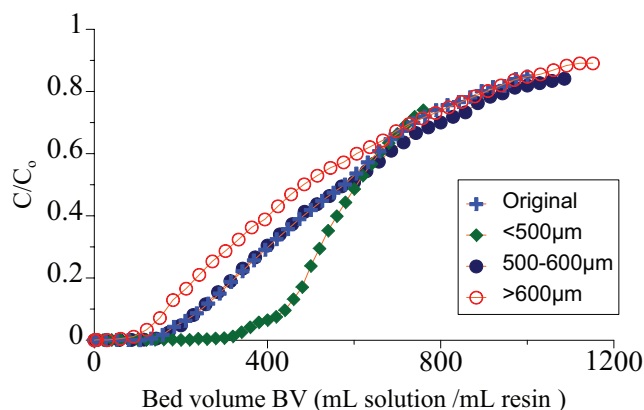


Fig. 6. Effect of resin size for the Amberlite IRA743 resin packed in a column.

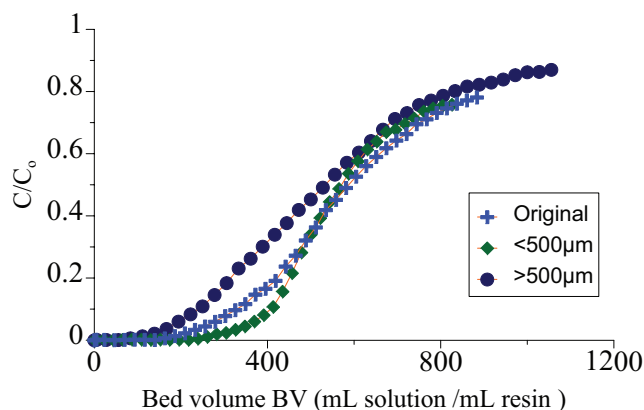


Fig. 7. Effect of resin size for the Purolite S108 resin packed in a column.

breakthrough volume of 400 BV and was steeper. On the contrary, for the $>600 \mu\text{m}$ resins, breakthrough occurred earlier and the breakthrough point was 150 BV.

With the Purolite S108 resin, breakthrough occurred later and the breakthrough curve was steeper for the $<500 \mu\text{m}$ resin, while the breakthrough curve obtained with the $>500 \mu\text{m}$ resin occurred earlier and was broadened compared with the original resin (Fig. 7). With the Diaion CBR05 resin, again, a similar effect was observed (Fig. 8). Breakthrough with resin size $<500 \mu\text{m}$ occurred later than the original resin, while the breakthrough curves with resins with size $500\text{--}600 \mu\text{m}$ and $>600 \mu\text{m}$ occurred earlier. Therefore, for the three resins, the smaller size $<500 \mu\text{m}$ gave higher volumes treated at breakthrough.

3.4. Influence of the type of resin in a packed column

The breakthrough curves obtained with the three original resins are shown in Fig. 9(a). Small differences were observed; in particular, breakthrough occurred slightly earlier for the Amberlite IRA743 resin. At higher volumes treated, the breakthrough curves obtained with the Amberlite IRA 743 and Purolite S108 resins became similar, while the one obtained with the Diaion CRB05 resin was flattened. Therefore, at the experimental conditions used, the Diaion CRB05 resin gave

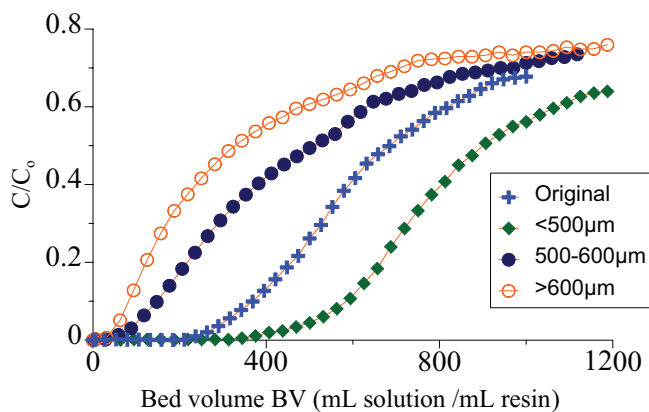
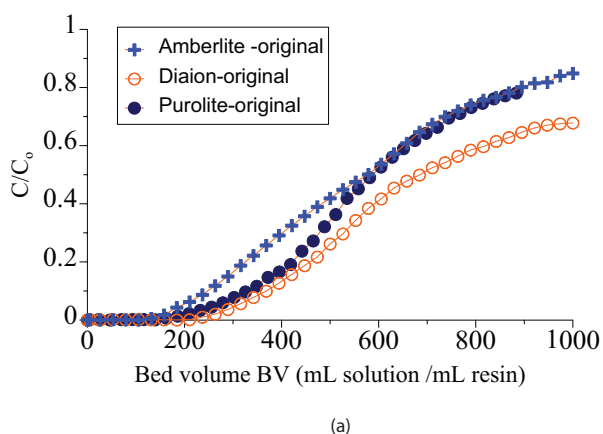


Fig. 8. Effect of resin size for the Diaion CRB05 resin packed in a column.



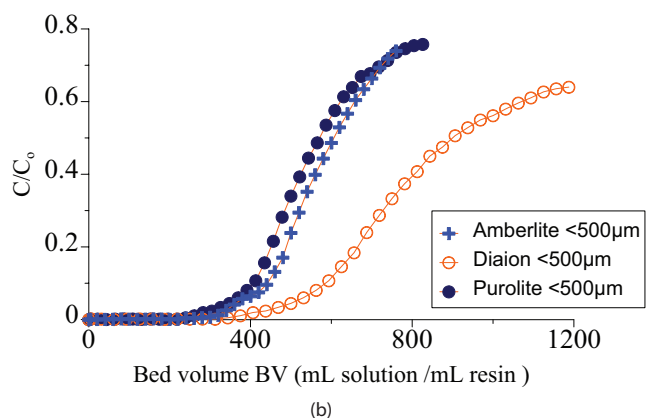
(a)

slightly better performance than the two other ones. Arias et al. [13] observed similar behavior when comparing three commercial resins: Amberlite IRA743, Purolite S108, and XU 43594.00, the beginning of the appearance of boron in the treated water occurring at very similar point.

For the three resins with the same particle size ($<500 \mu\text{m}$), the breakthrough curves are compared in Fig. 9(b). Breakthrough curves observed with the Amberlite IRA743 and Purolite S108 resin were very similar while the one obtained with the Diaion CRB05 resin was delayed and broadened. At this size, the Diaion CRB05 resin seems more efficient than the two other ones in terms of volume treated at breakthrough/volume of resin. This may be due to the fraction of smaller size (around $200\text{--}300 \mu\text{m}$) of the Diaion resin which was not present in the two other resins (Fig. 3(a)). However, the volume treated/mass of resin was higher for the Amberlite IRA743 resin than for the Diaion CRB05 resin (1 L/g instead of 0.85 L/g) (Table 2). This is due to the difference between resin volume/g, which were, respectively, equal to 5 and 3.2 mL for 2 g of Amberlite $<500 \mu\text{m}$ and Diaion CRB05 $<500 \mu\text{m}$ resins. Similar results were obtained with the $500\text{--}600 \mu\text{m}$ resins and the largest resin ($>600 \mu\text{m}$).

3.5. Comparison of column and hybrid sorption/MF

In this section, a comparison between the hybrid sorption/MF process and the column is realized. Fig. 10 shows the breakthrough curves obtained with the two processes. Experimental conditions and results are summarized in Table 3. The resin tested was the Amberlite IRA743 resin. For the column experiment, the resin size was $<500 \mu\text{m}$, which gave the sharper breakthrough curve, for the hybrid system, the resin size was $40\text{--}60 \mu\text{m}$. Indeed, the smallest size $40\text{--}60 \mu\text{m}$ was not used in the column due to the high pressure generated, but in the hybrid process where the transmembrane pressure driving the process is much lower. Other parameters values (membrane pore size, transmembrane pressure, etc.) were taken from our previous study [21] as they gave optimal breakthrough curve. On Fig. 10(a), it can be seen that similar breakthrough curves were obtained with the column and the hybrid system. Using the hybrid sorption/MF process, the breakthrough curve increased progressively after breakthrough similarly to the column breakthrough curve, although



(b)

Fig. 9. Effect of the resin type in a column: (a) with original resins and (b) resins with particle size $<500 \mu\text{m}$.

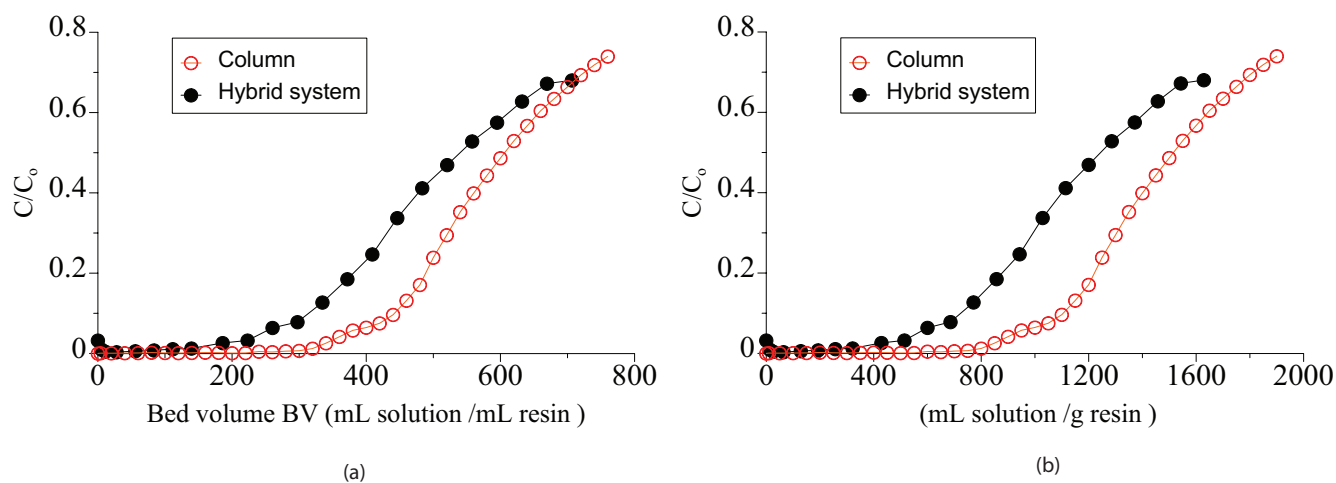


Fig. 10. Comparison of boron removal in column and hybrid sorption/MF system. Experimental conditions are given in Table 3. (a) Breakthrough curves vs. bed volume (mL solution/mL resin) and (b) volume treated (mL) divided by the mass of resin (g).

Table 3

Experimental conditions and results for the comparison between the ion-exchange/MF system and the ion-exchange column

	Experimental conditions	Results
Hybrid process	10 g Amberlite IRA743 (40–60 μm) Treated volume of boron solution = 15 L, $C_0 = 5 \text{ mg/L}$ V (10 g) = 23.05 mL Membrane 0.1 μm Transmembrane pressure PTM = 1 bar $Q = 42.8 \text{ mL/min}$	Time necessary for treatment of 15 L = 6.5 h $C = 0.32 \text{ mg/L}$ at $t = 160 \text{ min}$ (BV = 300)
Column	2 g Amberlite IRA743 (<500 μm) Treated volume of boron solution = 3.8 L, $C_0 = 5 \text{ mg/L}$ V (2 g) = 5 mL Pressure = 0.09 Mpa (0.9 bar) $Q = 2 \text{ mL/min}$	Time necessary for treatment of 3.8 L = 31.6 h $C = 0.32 \text{ mg/L}$ at $t = 1,000 \text{ min}$ (BV = 400)

breakthrough occurred earlier with the hybrid system. Indeed, the concentration 0.3 mg/L was reached after 300 and 400 BV, with the hybrid system and the column, respectively.

Besides, the flow rate obtained in the hybrid system (42 mL/min) was around 20 times higher than the one used in the column (2 mL/min) (Table 3). Indeed, the hybrid process allowed using resin with much smaller size (40–60 μm) than in a column, sorption was then much faster and permeate free of boron was obtained at high flow rate. As indicated in Table 3, a higher volume was treated during a shorter time with the hybrid process. When the breakthrough volume was divided by the resin mass (instead of the resin volume), the comparison between the two breakthrough curves was similar (Fig. 10(b)). The higher flow rates obtained in the hybrid system could be of interest in an industrial plant of seawater treatment.

In addition, for the hybrid process, the permeate flow rate was measured vs. time (data not shown). After a small decrease during the first 15 min corresponding to the formation of a cake layer at the membrane surface, the permeate flow rate was found constant during all the experiment suggesting low membrane fouling. This result was explained by

the resin size (40–60 μm) which was much larger than the membrane pores size and by the very small size of borate ions [21]. Thus, both resins and borate ions hardly cause membrane fouling.

4. Conclusion

Ion-exchange resins are commonly used for boron removal from seawater, geothermal water, and wastewater. They are often packed in large columns and have to be operated at small flow rates. In this study, we investigated the effect of resin size for three commercial resins (Amberlite IRA743, Diaion CRB05, and Purolite S108) in batch, column, and in a hybrid sorption/MF process. The breakthrough curves obtained in a column and in the hybrid ion-exchange/MF process were compared for the Amberlite IRA743 resin. Due to the smaller size of resin used in the hybrid process (40–60 μm), the process efficiency was improved: similar breakthrough curves were obtained while the flow rate was 20 times higher for the hybrid system. These results support the idea that the hybrid ion-exchange/MF technique could be a possible alternative to classical columns.

Acknowledgments

We thank the Libyan Embassy in France for providing a grant to Mrs Assma Alharati during her PhD thesis. We also thank Laurence Retailleau-Mével and Antoinette Boréave (IRCELYON, Villeurbanne, France) for the BET measurements.

References

- [1] J. Wolska, M. Bryjak, Methods for boron removal from aqueous solutions – a review, *Desalination*, 310 (2013) 18–24.
- [2] N. Hilal, G.J. Kim, C. Somerfield, Boron removal from saline water: a comprehensive review, *Desalination*, 273 (2011) 23–35.
- [3] World Health Organization, Guidelines for Drinking-water Quality, 4th ed., 2011.
- [4] Y. Xu, J.-Q. Jiang, Technologies for boron removal, *Ind. Eng. Chem. Res.*, 47 (2008) 16–24.
- [5] M.-O. Simonnot, C. Castel, M. Nicolai, C. Rosin, M. Sardin, H. Jauffret, Boron removal from drinking water with a boron selective resin: is the treatment really selective ?, *Water Res.*, 34 (2000) 109–116.
- [6] N. Kabay, S. Sarp, M. Yuksel, Ö. Arar, M. Bryjak, Removal of boron from seawater by selective ion exchange resins, *React. Funct. Polym.*, 67 (2007) 1643–1650.
- [7] N. Öztürk, T.E. Köse, Boron removal from aqueous solutions by ion-exchange resin: batch studies, *Desalination*, 227 (2008) 233–240.
- [8] E.B. Simsek, U. Beker, B.F. Senkal, Predicting the dynamics and performance of selective polymeric resins in a fixed bed system for boron removal, *Desalination*, 349 (2014) 39–50.
- [9] N.B. Darwish, V. Kochkodan, N. Hilal, Boron removal from water with fractionized Amberlite IRA743 resin, *Desalination*, 370 (2015) 1–6.
- [10] A.E. Yilmaz, R. Boncukcuoglu, M.T. Yilmaz, M.M. Kocakerim, Adsorption of boron from boron-containing wastewaters by ion exchange in a continuous reactor, *J. Hazard. Mater.*, B117 (2005) 221–226.
- [11] N. Kabay, S. Sarp, M. Yuksel, M. Kitis, H. Koseoglu, Ö. Arar, M. Bryjak, R. Semiat, Removal of boron from SWRO permeate by boron selective exchange resins containing N-methyl glucamine groups, *Desalination*, 223 (2008) 49–56.
- [12] I.Y. Ipek, N. Kabay, M. Yüksel, Modeling of fixed bed column studies for removal of boron from geothermal water by selective chelating ion exchange resins, *Desalination*, 310 (2013) 151–157.
- [13] M.F.C. Arias, L.V.i Bru, D.P. Rico, P.V. Galvañ, Comparison of ion exchange resins used in reduction of boron in desalinated water for human consumption, *Desalination*, 278 (2011) 244–249.
- [14] T.E. Köse, N. Öztürk, Boron removal from aqueous solutions by ion-exchange resin: column sorption–elution studies, *J. Hazard. Mater.*, 152 (2008) 744–749.
- [15] R. Boncukcuoglu, A.E. Yilmaz, M. Muhtar Kocakerim, M. Copur, An empirical model for kinetics of boron removal from boron containing wastewaters by ion exchange in a batch reactor, *Desalination*, 160 (2004) 159–166.
- [16] I.Y. Ipek, R. Holdich, N. Kabay, M. Bryjak, M. Yuksel, Kinetic behaviour of boron selective resins for boron removal using seeded microfiltration system, *React. Funct. Polym.*, 67 (2007) 1628–1634.
- [17] M. Bryjak, J. Wolska, I. Soroko, N. Kabay, Adsorption-membrane filtration process in boron removal from first stage seawater RO permeate, *Desalination*, 241 (2009) 127–132.
- [18] N. Kabay, P. Köseoğlu, E. Yavuz, Ü. Yüksel, M. Yüksel, An innovative integrated system for boron removal from geothermal water using RO process and ion exchange-ultrafiltration hybrid method, *Desalination*, 316 (2013) 1–7.
- [19] N. Kabay, I. Yilmaz-Ipek, I. Soroko, M. Makowski, O. Kirmizisakal, S. Yag, M. Bryjak, M. Yuksel, Removal of boron from Balcova geothermal water by ion exchange-microfiltration hybrid process, *Desalination*, 241 (2009) 167–173.
- [20] N.B. Darwish, V. Kochkodan, N. Hilal, Microfiltration of micro-sized suspensions of boron-selective resin with PVDF membranes, *Desalination*, 403 (2017) 161–171.
- [21] A. Alharati, Y. Swesi, K. Fiyat, C. Charcosset, Boron removal in water using a hybrid membrane process of ion exchange resin and microfiltration without continuous resin addition, *J. Water Process Eng.*, 17 (2017) 32–39.
- [22] AFNOR, Dosage du bore par spectrométrie d'absorption moléculaire, Méthodes à l'azométhine H, in *Qualité de l'eau, Norme ANFOR T 90-041*, 2001, 395–398.